NeuroImage 63 (2012) 1775–1781

Contents lists available at SciVerse ScienceDirect

NeuroImage

journal homepage: www.elsevier.com/locate/ynimg

Recovery of the default mode network after demanding neurofeedback training occurs in spatio-temporally segregated subnetworks

Dimitri Van De Ville [a,b,*], Permi Jhooti [c,d], Tanja Haas [c], Rotem Kopel [a,b], Karl-Olof Lovblad [e], Klaus Scheffler [f,g], Sven Haller [e]

[a] Department of Radiology and Medical Informatics, University of Geneva, Switzerland
[b] Institute of Bioengineering, Ecole Polytechnique Fédérale de Lausanne, Switzerland
[c] Institute of Radiology, University Hospital Basel, Switzerland
[d] Institut Design- und Kunstforschung, FHNW, Basel, Switzerland
[e] Service neuro-diagnostique et neuro-interventionnel DISIM, University Hospitals of Geneva, Switzerland
[f] Max Planck Institute for Biological Cybernetics, MRC Department, Tübingen, Germany
[g] Department for Biomedical Magnetic Resonance, University of Tübingen, Tübingen, Germany

ARTICLE INFO

Article history:
Accepted 23 August 2012
Available online 30 August 2012

Keywords:
Default mode network
Resting state
fMRI
Functional connectivity
Networks
ICA

ABSTRACT

The default mode (DM) network is a major large-scale cerebral network that can be identified with functional magnetic resonance imaging (fMRI) during resting state. Most studies consider functional connectivity networks as stationary phenomena. Consequently, the transient behavior of the DM network and its subnetworks is still largely unexplored. Most functional connectivity fMRI studies assess the steady state of resting without any task. To specifically investigate the recovery of the DM network during the transition from activation to rest, we implemented a cognitively demanding real-time fMRI neurofeedback task that targeted down-regulation of the primary auditory cortex. Each of twelve healthy subjects performed 16 block-design fMRI runs (4 runs per day repeated on 4 days) resulting 192 runs in total. The analysis included data-driven independent component analysis (ICA) and high-resolution latency estimation between the four components that corresponded to subnetworks of the DM network. These different subnetworks reemerged after regulation with an average time lag or 3.3 s and a time lag of 4.4 s between the first and fourth components; i.e., the DM recovery first shifts from anterior to posterior, and then gradually focuses on the ventral part of the posterior cingulate cortex, which is known to be implicated in internally directed cognition. In addition, we found less reactivation in the early anterior subnetwork as regulation strength increased, but more reactivation with larger regulation for the late subnetwork that encompassed the ventral PCC. This finding confirms that the level of task engagement influences inversely the subsequent recovery of regions related to attention compared to those related to internally directed cognition.

Introduction

Deeper understanding of the brain's intrinsic functional organization is one of the main aims of functional magnetic resonance imaging (fMRI) at resting state (Biswal et al., 1995; Fox and Raichle, 2007). The spontaneous fluctuations of the blood oxygenation level dependent (BOLD) signal can be used to measure functional connectivity between different voxels or regions in the brain, and thus establish intrinsic large-scale functional networks. Such functional connectivity analysis gives insight about functional integration, and measuring it at resting state does not require a specific experimental setup or paradigm in contrast to conventional stimulus-related fMRI; this has a high potential for clinical applications (Broyd et al., 2009; Damoiseaux et al., 2008).

The "default-mode" (DM) network is one of the prototypical resting-state networks; i.e., it can be identified as the network that "deactivates" compared to the task baseline, or by using functional connectivity analysis (Damoiseaux et al., 2006; Fox and Raichle, 2007; Greicius et al., 2003; Laird et al., 2011). While it is known that the DM network restores during the transition from activation to rest, and that its deactivation is not the same for all tasks, little is known about the temporal properties of this recovery, in particular with respect to DM subnetworks.

Functional connectivity is defined statistical dependence between different voxels or regions and mostly measured by temporal correlation (Friston, 1994). Consequently, most studies assess the steady state of resting and thus assume stationarity. However, recent evidence suggests that functional connectivity can be modulated spontaneously

Abbreviations: DM, default mode; fc, functional connectivity; fMRI, functional magnetic resonance imaging; ICA, independent component analysis; BOLD, blood oxygenation level dependent; vmPFC, ventromedial prefrontal cortex; dmPFC, dorsomedial prefrontal cortex; Prec, precuneus; PCC, posterior cingulate cortex; IPL, inferior parietal lobule; TC, temporal cortex; HF+, parahippocampal cortex.

* Corresponding author at: Institute of Bioengineering, Ecole Polytechnique Fédérale de Lausanne, Switzerland.
E-mail address: Dimitri.VanDeVille@epfl.ch (D. Van De Ville).

1053-8119/$ – see front matter © 2012 Elsevier Inc. All rights reserved.
http://dx.doi.org/10.1016/j.neuroimage.2012.08.061

(Raichle, 2010), by exogenous stimulation (Buchel et al., 1999) and by learning (Bassett et al., 2011; Lewis et al., 2009).

Here we assessed the recovery of the DM network following a demanding cognitive task. In particular, we used a real-time fMRI (rt-fMRI) neurofeedback paradigm (deCharms, 2007; Weiskopf et al., 2003) to let the subject down-regulate brain activity in the right primary auditory cortex. Previous work has shown that the suppression of the DM network during task is proportional to its level of cognitive demand or task difficulty, e.g. (Leech et al., 2011). In our case, we expect a strong de-activation of DM network during the task, followed by recovery in subsequent resting epochs. In addition, we use the regulation strength as measured in the auditory target region as a surrogate for task engagement. To obtain robust assessment of the recovery of the DM network, each subject performed 4 fMRI runs per day (session), which were repeated on 4 training days resulting in 16 sessions per subject, or 192 sessions in total. First, we made use of data-driven independent component analysis (ICA) to identify various temporally-coherent functional networks, and, in particular, four distinct DM subnetworks. For each of these components, we then investigated the time-lag differences and found statistically significant evidence for a specific sequence of how the DM subnetworks come back "online". Finally, we found differences in correlation of the activity in these subnetworks and regulation strength, which brings new evidence to the neurophysiological DM components.

Materials and methods

Subjects

Twelve healthy right-handed individuals participated for monetary compensation after giving informed consent approved by the local Ethics Committee. None suffered from current or prior neurological or psychiatric impairments or claustrophobia. Audition was normal. Mean age of participants was 28.37 y (range 24–33 y).

Task procedure

The rt-fMRI neurofeedback experimental was similar to a previous study (Haller et al., 2010). Each subject had 4 sessions performed in 4 different days, while a session was designed as the following protocol: First, a standard fMRI auditory block-design paradigm was performed to identify the individual primary auditory area with 20 s ON, 20 s OFF, (5 repetitions) bilateral auditory stimulation using a sine tone of 1000 Hz pulsating at 10 Hz that is known to induce a strong and long-lasting BOLD response (Haller et al., 2006; Seifritz et al., 2002). Second, 4 rt-fMRI neurofeedback training runs were performed. Each run started with a 30 s baseline period followed by a block-design alternating between down-regulation (60 s) and no-regulation periods (30 s) repeated 4 times. Visual feedback was provided as a moving line graph. The visual feedback was provided during the entire run. The participants were informed about the data processing delay of about 1 s and of the intrinsic physiological hemodynamic response delay of about 6 s. During the down-regulation periods, the same pulsating sine tone of 1000 Hz was provided as auditory stimulation. Each training day (session) included 4 runs performed sequentially. Each participant performed 4 training days (sessions) using the same protocol (with approximately 1 week interval). This leads to a total of 16 runs per subject. We used the Turbo BrainVoyager software package (www.brainvoyager.com) in combination with in-house Matlab (www.mathworks.com) scripts for online data analysis and feedback presentation.

fMRI data acquisition

Functional images were acquired on 3 T whole-body MR scanner with a standard 12-channel head coil (Siemens Magnetom Verio, Siemens Erlangen, Germany). A standard Echo-Planar Imaging (EPI) sequence was used: Echo time (TE) 40 ms, repetition time (TR) 2000 ms, matrix size 64×64, effective voxel size $3\times3\times3$ mm. Additionally, we acquired an anatomical T1-weighted whole brain Magnetization Prepared Rapid Gradient Echo (MPRAGE), matrix size 256×256, 176 partitions, 1 mm^3 isotropic voxels, 26 slices with 3-mm thickness. The cranial part of the cerebrum was not fully covered in all subjects.

Pre-processing and GLM analysis

Pre-processing was performed using the SPM8 software (Wellcome Department of Imaging Neuroscience, London, UK). First, all functional volumes were spatially realigned to the first volume, normalized into MNI space (Montreal Neurological Institute, resampled voxel size: $2\times2\times2$ mm) by using cubic B-spline interpolation, and smoothed using an isotropic Gaussian spatial kernel (FWHM 6 mm).

For post-hoc statistical analysis of the down-regulation, we have performed 1st level analysis GLM. The design matrix of the general linear model (GLM) was set up with 16 identical blocks on the diagonal, each contains a constant and a regressor that modeled the BOLD response associated to the design of a single run (base line and 4 alternating blocks of down regulation). Data were high-pass filtered to a cut-off of 1/128 Hz and serial correlation was modeled by the autoregressive model of order 1. The analysis was performed at the group level by a 2nd level design that used the contrasts of all subjects at all sessions and all runs ($12\times4\times4=192$ contrasts), the design matrix was set with 12 identical blocks on the diagonal, each block was with a constant and a linear modulation as a function of training day. Statistical maps for the modulation were obtained using a t-test for the corresponding contrast and corrected for multiple comparisons using family-wise error (FWE) at $p=0.05$.

Independent component analysis

We used group spatial ICA (Calhoun et al., 2001) to decompose the data into independent components using the GIFT toolbox (http://icatb.sourceforge.net/). We applied ICA to the group data by concatenating all sessions and all runs of all subjects. The dimensionality at the 1st level principal component analysis was chosen to be 80, which leads to time-courses that are close to the original data since most of the original signal's variance can still be explained in this subspace (Allen et al., 2012). For the 2nd level component analysis, we used the ICASSO algorithm (Himberg et al., 2004) to assess the consistency of the components (i.e., how robust they are over 10 runs of ICA), ICASSO returns a stability (quality) index (Iq) for each estimated cluster. This gives a quality ranking of the different independent components, known as the Iq plot. We checked the Iq plot for different numbers of components and selected the number of components as high as possible where the Iq plot is still stable (close to one). This led us to estimate the final number of components to be 25. ICA decomposes the data into several temporally coherent functional networks (independent components, ICs). These maps can be extracted for each run with associated time-courses. We scaled the intensities at each voxel to spatial z-scores, and then performed a one-sample t-test over all runs/sessions/subjects to determine the significant contributions for each IC. We manually selected 4 out of the 25 ICs to be DM subnetworks.

High-resolution latency analysis

We submitted the associated time-courses of the ICs for all runs to a latency analysis. We first averaged for each time-course over all 4 blocks (i.e., the 4 down-regulation and 4 resting blocks) into one segment that contains the end of a down-regulation epoch, followed by the resting epoch, and the beginning of a regulation epoch as illustrated in Fig. 3a. Specifically, the latency between two time-courses for

different ICs, averaged over runs, was determined by extracting the cross-correlation peak with micro-time resolution of TR/32, which was obtained using Fourier-domain upsampling that corresponds to sinc-interpolation in the temporal domain. Under the null hypothesis that no time-lag was present between the ICs, we randomly exchanged time-courses between the ICs and recomputed the cross-correlation peak between the time-courses averaged per IC to generate the null-distribution of the time-lag in a non-parametric way. Using 1000 permutations, we looked for evidence that the three pair-wise comparisons are significant at $p<0.05$, corrected for multiple comparisons. In addition, we applied the analysis for the time-courses with slight temporal smoothing (Gaussian kernel FWHM = 8.5 s). The plots of the time-courses always show the temporally smoothed versions.

Relationship with regulation strength

As a measure of activity for the ICs, we computed the "total activation" as the sum of absolute values of the time-courses for each block; i.e., a block consisted of a regulation epoch followed by a resting epoch as explained above, leading to 4 blocks per run. We computed this measure for the four DM subnetworks, as well the IC comprising the primary auditory network that was targeted. For the latter network, the activation measure was interpreted as the inverse of regulation strength; i.e., a lower value corresponds to stronger *down*-regulation, while a higher value to weaker down-regulation. We then removed the mean total activation per subject (over runs and sessions) and performed linear regression between the total activation in the auditory IC and the DM subnetworks (4 blocks × 4 runs × 4 sessions × 12 subjects), and submitted the slope to a standard one-sample t-test.

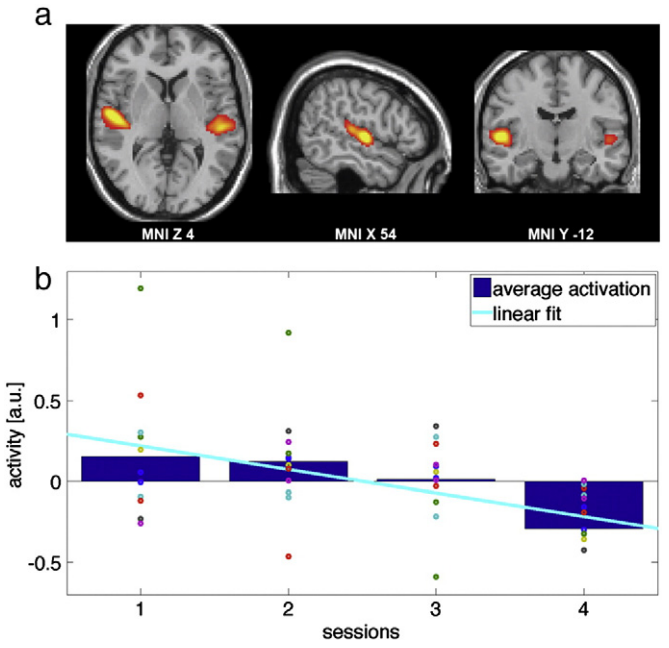

Fig. 1. (a) General linear model analysis of the real time fMRI runs confirms the successful voluntary down-regulation of the primary auditory area by means of neurofeedback (group results, thresholded at $t>15$ for illustrative purposes). (b) The BOLD signal contrast at the peak voxel (X 54,Y −12,Z 4) is consistent with the neurofeedback target region in the right auditory area. We show the regulated level as a function of session; the linear fit shows that down-regulation is improved over sessions. The subject-wise values are plotted as markers in the background.

Results

Using post-hoc GLM analysis, we showed that rt-fMRI leads to a successful down-regulation of brain activity levels in the target region in the right primary auditory cortex (Fig. 1a). Our second level analysis confirms a significant improvement in down-regulation as a regulation improves (Fig. 1b). Then, using ICA, we were able to identify four DM subnetworks (Fig. 2 and Table 1). The time-courses of these ICs were then submitted to the latency analysis (Fig. 3a), which resulted into the following estimates: 2.1 s (DMN 1–2); 2.3 s (DMN 1–3); 4.4 s (DMN 1–4). Comparable results were obtained with temporal smoothing. The latency that can be expected by chance as established by the permutation test between −1.1 to 1.1 s (95% confidence interval). Finally, the relationship between activity in the auditory network and the DM subnetworks is shown in Fig. 3b.

Discussion

Our results reveals how the DM network recovers after a cognitively demanding rt-fMRI task, following a specific spatio-temporal sequence of its subnetworks; i.e., activity first proceeds from anterior to posterior, and then refocuses from the dorsal toward the ventral part of the PCC, which is one of the cortical hubs of the brain (Hagmann et al., 2008). We will first briefly revisit the concept of the DM network. Then, we discuss the partitioning of the DM network and its dynamic recovery in light of recent studies on temporal organization of the DM network and, finally, with respect to local differences in neurovascular coupling.

Functional connectivity and the default mode network

The notion of a "default mode" of the brain at rest was introduced by Raichle et al. in 2001 (Raichle et al., 2001), and further elucidated as a "network" by Greicius et al. (2003). The DM network consists of a core network including ventral and dorsal medial prefrontal cortex (vmPFC, dMPFC), precuneus (Prec), posterior cingulate cortex (PCC) and the inferior parietal lobule (IPL). Some authors additionally consider the temporal cortex (TC) and the parahippocampal cortex (HF+) as associated areas. In the absence of any stimulation paradigm, the DM network can be identified using functional connectivity, either using the PCC as a seed region in correlation analysis, or using ICA to decompose the data in a set of temporally coherent networks (Damoiseaux et al., 2006; Fox and Raichle, 2007; Greicius et al., 2003; Laird et al., 2011). In addition, the DM network's functional connectivity is supported by structural connectivity (Greicius et al., 2009; Teipel et al., 2010; van den Heuvel et al., 2008). Despite the established functional and structural connectivity of the DM network, its neurophysiological interpretation remains to date more controversial (Morcom and Fletcher, 2007; Raichle, 2006; Raichle and Snyder, 2007).

Conventional resting-state analysis assumes steady-state functional connectivity during runs without any task, and thus DM network dynamics, reflecting, for example, short-term "transition" effects, can provide additional insights in the function and these networks and their interdependencies. Recently, non-stationary properties of brain networks have started to receive interest from the neuroimaging community, see, for example Smith et al. (2012). Here we propose a data-driven analysis without preselecting any neither brain regions nor timing. The time-courses of the ICs corresponding to DM subnetworks reveal information about magnitude and phase, which characterizes the recovery following a very cognitively demanding neurofeedback task. Finally, the regulation strength of the rt-fMRI neurofeedback gives a measure of task engagement directly extracted from the imaging data.

Partitioning of the DM network into subnetworks

In the majority of functional connectivity studies, the DM network is identified as a single large-scale network. Hampson et al. (2006) looked into connectivity between PCC and medial frontal regions and its modulation during rest and a working memory task. They

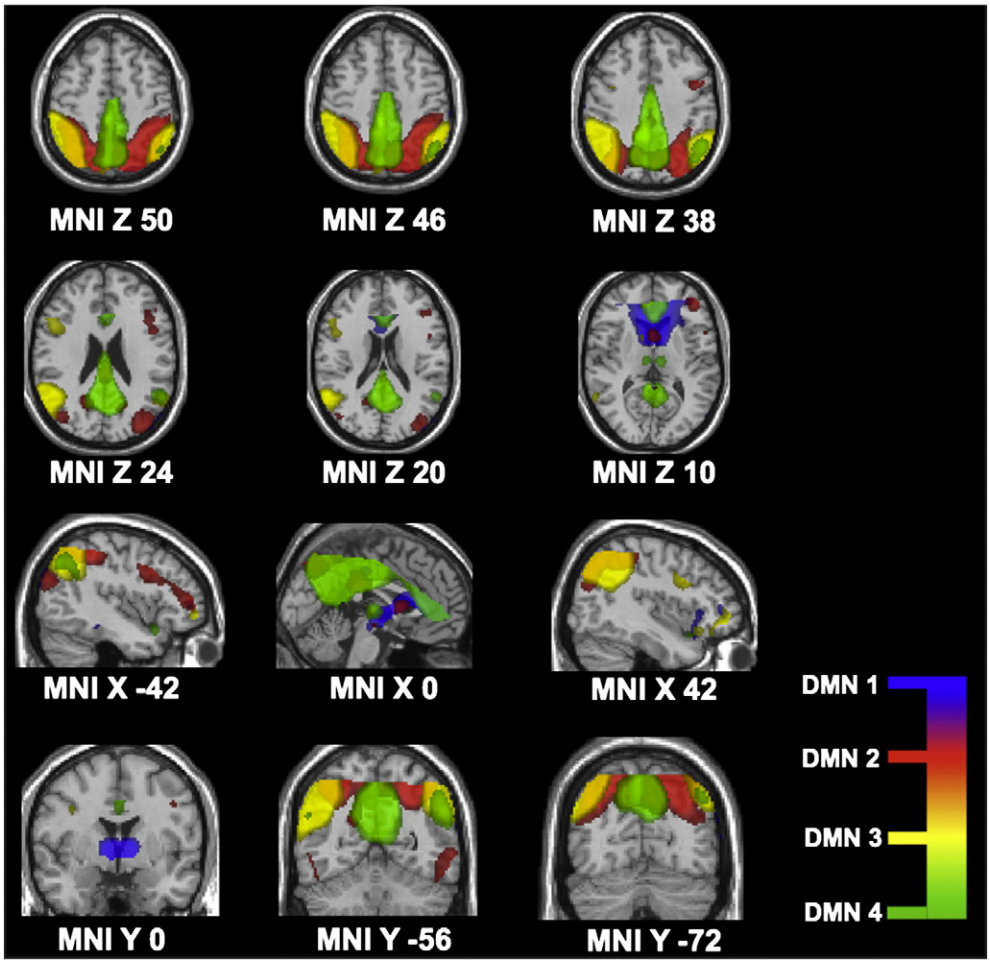

Fig. 2. Whole-brain results from a data-driven ICA analysis of resting-state fMRI data. The four ICs that correspond to DM subnetworks are shown in the axial, sagittal, and coronal views. According to the latency analysis on the associated time-courses (see Fig. 3a), the colors of the networks, according to the order of recovery are blue, red, yellow, and green, respectively.

observed a positive correlation between functional connectivity and the performance at the working memory task, suggesting a DM subnetwork that may facilitate cognitive performance. Uddin et al. (2009) studied seed-region connectivity analysis for PCC and vmPFC. Networks that positively correlate when using these regions as seeds largely overlapped; however, the anti-correlated networks for these seeds showed striking differences. A recent network connectivity study demonstrated a functional segregation of the DM network based on a combination of spatial and temporal ICA (Smith et al., 2012); in particular, the authors showed that the PCC hub, during rest, becomes alternately part of different networks. In a more clinical context, Damoiseaux et al. showed altered connectivity in parts of the DM networks as Alzheimer's disease progresses (Damoiseaux et al., 2012).

Table 1
List of regions that constitute the four ICs corresponding the DM subnetworks.

Subnetwork	Brain regions
DMN 1	Bilateral anterior cingulate cortex
	Bilateral vmPFC
	Bilateral dmPFC
DMN 2	Bilateral posterior cingulate cortex
	Bilateral precuneus
	Bilateral parahippocampal cortex
	Bilateral middle/inferior frontal gyrus
	Bilateral superior/inferior parietal lobule
	Bilateral lateral occipital cortex
	Bilateral anterior insula
DMN 3	Bilateral posterior cingulate cortex
	Bilateral precuneus
	Bilateral anterior cingulate cortex
	Bilateral vmPFC
	Bilateral superior/inferior parietal lobule
DMN 4	Bilateral posterior cingulate cortex
	Bilateral precuneus
	Bilateral inferior parietal lobule
	Bilateral anterior cingulate cortex
	Bilateral inferior frontal gyrus
	Bilateral parahippocampal cortex
	Bilateral thalamus

In this work, we identified four different subnetworks of the DM network, which means that their underlying dynamics are sufficiently dissimilar such that ICA can separate them into different components. Based on the latencies between the time-courses of these subnetworks (Fig. 3a), it is likely that their separability is mainly driven by the differences during the recovery in the resting epoch. The first subnetwork (DMN 1) includes anterior regions, and, from the positive correlation with activation in the auditory component, and consequently negative correlation with *down*-regulation strength, see Fig. 3b, we find that its recovery is weaker after stronger regulation, which presumably corresponds to higher recruitment of this DM subnetwork when cognitive demand increases. The second subnetwork mainly encompasses superior parietal regions; it is not modulated by regulation strength. Next, the PCC, commonly identified as the core of the DM network, appears as part of DMN 3 and 4. The dorsal part of the PCC, which is reportedly implicated in more externally directed cognition and related to "task-

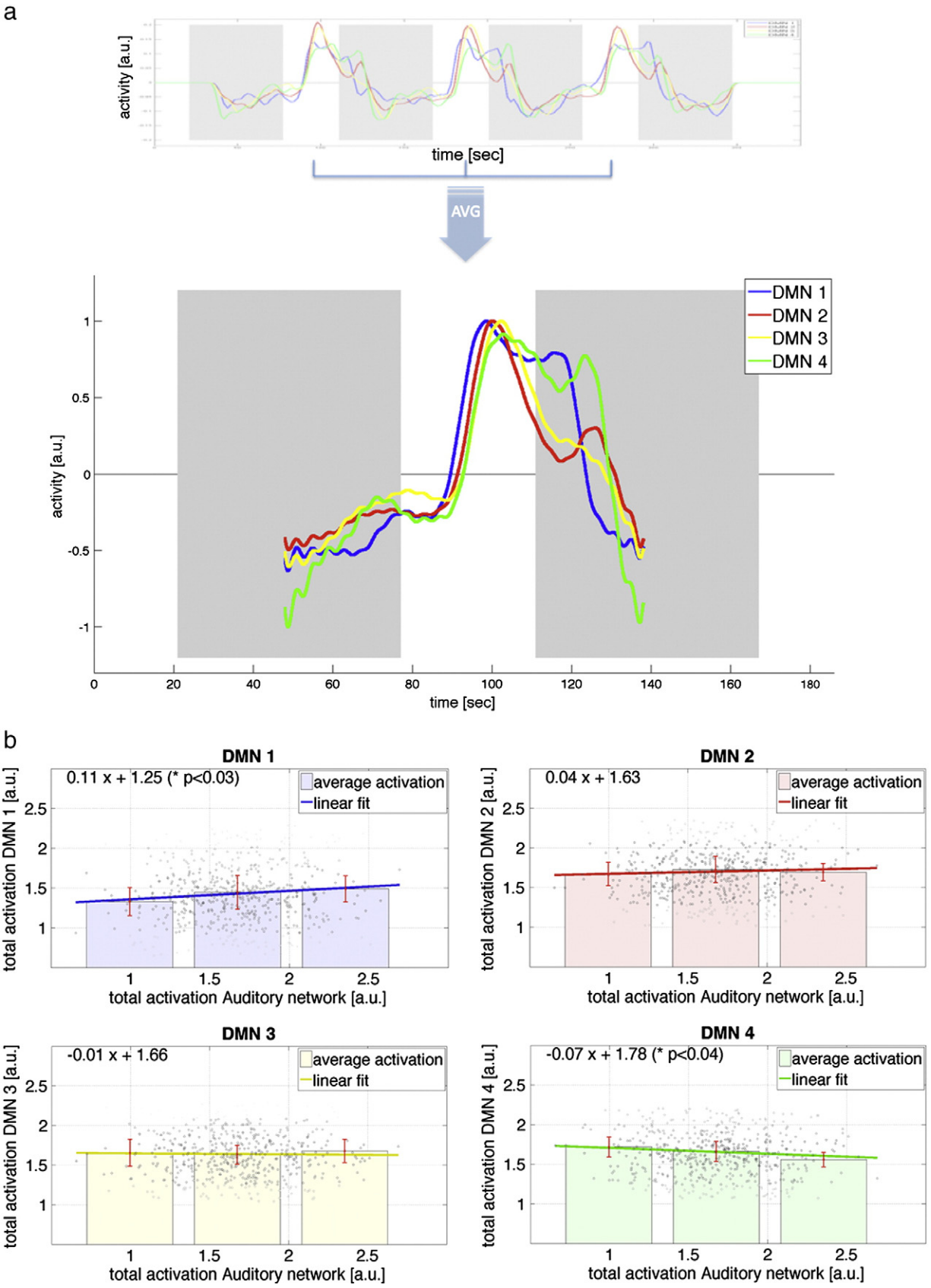

Fig. 3. (a) Average time-courses of one block of the DM subnetworks shown in Fig. 2. The average was performed over all blocks, runs, session, and subjects. (b) Scatter plots and correlation analysis between the activation in the auditory component and the DM subnetworks. Each dot corresponds to a block. Linear regression is performed on the complete cloud of dots. For visualization purposes, we show the total activation binned according to three levels of activation in the auditory component, and we modulated the intensity of the dots according to their excursion in the DM subnetwork activity.

positive" regions (Leech et al., 2011), is part of DMN 3; again, there is no significant modulation with regulation strength. However, the ventral part of the PCC belongs to DMN 4 and is implicated in more internally directed cognition (Shannon and Buckner, 2004). Functional-anatomic correlates of memory retrieval suggest nontraditional processing roles for multiple distinct regions within posterior parietal cortex (Buckner et al., 2008; Leech et al., 2011; Shannon and Buckner, 2004). The degree of activation of DMN 4 is *inversely* proportional with activation in the auditory component, which indicates that stronger cognitive demands increase the re-establishment of this subnetwork. It is interesting to relate this finding with the results of Eichele et al. (2008), who demonstrated that coincident decrease of deactivation in DM regions, together with decrease of activation in task-related regions, raised the probability of future errors. The authors discuss this dysfunction as "systematic maladjustment in cognitive control systems" of the described network that develops slowly over time. In our case, the recovery of the subnetworks seems to be differentially affected by regulation. The anterior part (DMN 1) is known to be primarily related to attentional aspects (Weissman et al., 2006) but it is also part of the saliency network (Fox et al., 2006; Seeley et al., 2007) and has a role in switching between DM and executive function (Sridharan et al., 2008). Our finding that this subnetwork is the first one to recover and less so as regulation becomes stronger, confirms its switching role and implication in attention and executive control recruited in a regulation task. The ventral PCC (DMN 4) is linked to internally directed thoughts, which reactivates stronger after high task engagement. Finally, it is also compelling that the late DMN 4 is most focused on the PCC, which confirms the notion that the PCC is echoing activity from other brain networks (Leech et al., 2012), but modulated by task intensity. Interestingly, the time-courses of the different subnetworks (Fig. 3a) show that DMN 4 indeed has the largest latency with respect to the most anterior subnetwork (DMN 1), not only during rest but also during regulation, however, we do not find a perfect "echo" but only a similar time-course.

Local differences in the cerebrovascular response

It is important to consider local differences in the neurovascular coupling as a potential confound for the observed delay in BOLD responses (Aguirre et al., 1998; Haller et al., 2007; Huettel and McCarthy, 2001; Saad et al., 2001). Initial studies typically reported differences in the delay of the local neurovascular response in the range of 1 s (Aguirre et al., 1998; Huettel and McCarthy, 2001; Saad et al., 2001). More recent investigations used the global BOLD response related to the vasodilation of carbon dioxide (CO_2) either by directly applying CO_2 (Blockley et al., 2011; Chang and Glover, 2009; Haller et al., 2006, 2008) or, indirectly, by means of hypoventilation (or breath holding) induced hypercapnia or hyperventilation induced hypocapnia (Bright et al., 2009; Rostrup et al., 2000). The estimated delay in the cerebrovascular response (CVR) is longer in particular in the cerebellum and in the central grey matter with a delay of approximately 2–4 s and clearly less variation between frontal and occipital cortex (Chang and Glover, 2009). Another study specifically investigated regional differences in the CVR delay and found an anterior-to-posterior gradient in latency in the range of 1 to a maximum of 2 s (Blockley et al., 2011). The total time latency of the four DM subnetworks was 4.4 s, which clearly exceeds the local variation of CVR. The delays between the three posterior subnetworks are much smaller (of the order of 1 s), but since they are partially overlapping in nearby regions supplied in the same vascular territory, it is very unlikely that these latencies have a purely CVR-related origin.

Conclusion

In summary, we demonstrated that DM network recovery following a demanding rt-fMRI task occurs in four different subnetworks with different time latencies. The subnetworks take up functionally different parts of the DM network, and two of them are modulated by task intensity as measured by the regulation strength in the auditory region that was targeted by the real-time fMRI neurofeedback task. One limitation of our study is that causality between the subnetworks cannot be established. In that respect, future investigations should ideally combine fMRI with other neuroimaging methods such as EEG. The further interpretation of the neurophysiological importance of the DM network and its subnetworks remains an important research topic.

Disclosure

No conflicts of interest.

Acknowledgments

This work has been supported in part by the Swiss National Science Foundation (under the grants 320030_127079/1 and PP00P2-123438) and in part by the Center for Biomedical Imaging (CIBM) of the EPFL and the Universities and Hospitals of Lausanne and Geneva. We thank all participants. We would like to thank Dr. Elena Allen and Prof. Tom Eichele for their invaluable help with the GIFT analysis.

References

Aguirre, G.K., Zarahn, E., D'esposito, M., 1998. The variability of human, BOLD hemodynamic responses. NeuroImage 8, 360–369.
Allen, E.A., Erhardt, E.B., Wei, Y., Eichele, T., Calhoun, V.D., 2012. Capturing inter-subject variability with group independent component analysis of fMRI data: a simulation study. NeuroImage 59, 4141–4159.
Bassett, D.S., Wymbs, N.F., Porter, M.A., Mucha, P.J., Carlson, J.M., Grafton, S.T., 2011. Dynamic reconfiguration of human brain networks during learning. Proc. Natl. Acad. Sci. U. S. A. 108, 7641–7646.
Biswal, B., Yetkin, F.Z., Haughton, V.M., Hyde, J.S., 1995. Functional connectivity in the motor cortex of resting human brain using echo-planar MRI. Magn. Reson. Med. 34, 537–541.
Blockley, N.P., Driver, I.D., Francis, S.T., Fisher, J.A., Gowland, P.A., 2011. An improved method for acquiring cerebrovascular reactivity maps. Magn. Reson. Med. 65, 1278–1286.
Bright, M.G., Bulte, D.P., Jezzard, P., Duyn, J.H., 2009. Characterization of regional heterogeneity in cerebrovascular reactivity dynamics using novel hypocapnia task and BOLD fMRI. NeuroImage 48, 166–175.
Broyd, S.J., Demanuele, C., Debener, S., Helps, S.K., James, C.J., Sonuga-Barke, E.J., 2009. Default-mode brain dysfunction in mental disorders: a systematic review. Neurosci. Biobehav. Rev. 33, 279–296.
Buchel, C., Coull, J.T., Friston, K.J., 1999. The predictive value of changes in effective connectivity for human learning. Science 283, 1538–1541.
Buckner, R.L., Andrews-Hanna, J.R., Schacter, D.L., 2008. The brain's default network: anatomy, function, and relevance to disease. Ann. N. Y. Acad. Sci. 1124, 1–38.
Calhoun, V.D., Adali, T., Pearlson, G.D., Pekar, J.J., 2001. A method for making group inferences from functional MRI data using independent component analysis. Hum. Brain Mapp. 14, 140–151.
Chang, C., Glover, G.H., 2009. Relationship between respiration, end-tidal CO2, and BOLD signals in resting-state fMRI. NeuroImage 47, 1381–1393.
Damoiseaux, J.S., Rombouts, S.A., Barkhof, F., Scheltens, P., Stam, C.J., Smith, S.M., Beckmann, C.F., 2006. Consistent resting-state networks across healthy subjects. Proc. Natl. Acad. Sci. U. S. A. 103, 13848–13853.
Damoiseaux, J.S., Beckmann, C.F., Arigita, E.J., Barkhof, F., Scheltens, P., Stam, C.J., Smith, S.M., Rombouts, S.A., 2008. Reduced resting-state brain activity in the "default network" in normal aging. Cereb. Cortex 18, 1856–1864.
Damoiseaux, J.S., Prater, K.E., Miller, B.L., Greicius, M.D., 2012. Functional connectivity tracks clinical deterioration in Alzheimer's disease. Neurobiol. Aging 33, 828.e19–828.e30.
deCharms, R.C., 2007. Reading and controlling human brain activation using real-time functional magnetic resonance imaging. Trends Cogn. Sci. 11, 473–481.
Eichele, T., Debener, S., Calhoun, V.D., Specht, K., Engel, A.K., Hugdahl, K., von Cramon, D.Y., Ullsperger, M., 2008. Prediction of human errors by maladaptive changes in event-related brain networks. Proc. Natl. Acad. Sci. U. S. A. 105, 6173–6178.
Fox, M.D., Raichle, M.E., 2007. Spontaneous fluctuations in brain activity observed with functional magnetic resonance imaging. Nat. Rev. Neurosci. 8, 700–711.
Fox, M.D., Corbetta, M., Snyder, A.Z., Vincent, J.L., Raichle, M.E., 2006. Spontaneous neuronal activity distinguishes human dorsal and ventral attention systems. Proc. Natl. Acad. Sci. U. S. A. 103, 10046–10051.
Friston, K.J., 1994. Functional and effective connectivity in neuroimaging: a synthesis. Hum. Brain Mapp. 2, 56–78.
Greicius, M.D., Krasnow, B., Reiss, A.L., Menon, V., 2003. Functional connectivity in the resting brain: a network analysis of the default mode hypothesis. Proc. Natl. Acad. Sci. U. S. A. 100, 253–258.

Greicius, M.D., Supekar, K., Menon, V., Dougherty, R.F., 2009. Resting-state functional connectivity reflects structural connectivity in the default mode network. Cereb. Cortex 19, 72–78.
Hagmann, P., Cammoun, L., Gigandet, X., Meuli, R., Honey, C.J., Wedeen, V.J., Sporns, O., 2008. Mapping the structural core of human cerebral cortex. PLoS Biol. 6, e159.
Haller, S., Wetzel, S.G., Radue, E.W., Bilecen, D., 2006. Mapping continuous neuronal activation without an ON–OFF paradigm: initial results of BOLD ceiling fMRI. Eur. J. Neurosci. 24, 2672–2678.
Haller, S., Klarhoefer, M., Schwarzbach, J., Radue, E.W., Indefrey, P., 2007. Spatial and temporal analysis of fMRI data on word and sentence reading. Eur. J. Neurosci. 26, 2074–2084.
Haller, S., Bonati, L.H., Rick, J., Klarhofer, M., Speck, O., Lyrer, P.A., Bilecen, D., Engelter, S.T., Wetzel, S.G., 2008. Reduced cerebrovascular reserve at CO2 BOLD MR imaging is associated with increased risk of periinterventional ischemic lesions during carotid endarterectomy or stent placement: preliminary results. Radiology 249, 251–258.
Haller, S., Birbaumer, N., Veit, R., 2010. Real-time fMRI feedback training may improve chronic tinnitus. Eur. Radiol. 20, 696–703.
Hampson, M., Driesen, N.R., Skudlarski, P., Gore, J.C., Constable, R.T., 2006. Brain connectivity related to working memory performance. J. Neurosci. 26, 13338–13343.
Himberg, J., Hyvarinen, A., Esposito, F., 2004. Validating the independent components of neuroimaging time series via clustering and visualization. NeuroImage 22, 1214–1222.
Huettel, S.A., McCarthy, G., 2001. Regional differences in the refractory period of the hemodynamic response: an event-related fMRI study. NeuroImage 14, 967–976.
Laird, A.R., Fox, P.M., Eickhoff, S.B., Turner, J.A., Ray, K.L., McKay, D.R., Glahn, D.C., Beckmann, C.F., Smith, S.M., Fox, P.T., 2011. Behavioral interpretations of intrinsic connectivity networks. J. Cogn. Neurosci. 23 (12), 4022–4037.
Leech, R., Kamourieh, S., Beckmann, C.F., Sharp, D.J., 2011. Fractionating the default mode network: distinct contributions of the ventral and dorsal posterior cingulate cortex to cognitive control. J. Neurosci. 31, 3217–3224.
Leech, R., Braga, R., Sharp, D.J., 2012. Echoes of the brain within the posterior cingulate cortex. J. Neurosci. 32, 215–222.
Lewis, C.M., Baldassarre, A., Committeri, G., Romani, G.L., Corbetta, M., 2009. Learning sculpts the spontaneous activity of the resting human brain. Proc. Natl. Acad. Sci. U. S. A. 106, 17558–17563.
Morcom, A.M., Fletcher, P.C., 2007. Does the brain have a baseline? Why we should be resisting a rest. NeuroImage 37, 1073–1082.
Raichle, M.E., 2006. Neuroscience. The brain's dark energy. Science 314, 1249–1250.
Raichle, M.E., 2010. Two views of brain function. Trends Cogn. Sci. 14, 180–190.
Raichle, M.E., Snyder, A.Z., 2007. A default mode of brain function: a brief history of an evolving idea. NeuroImage 37, 1083–1090 (discussion 1097–9).
Raichle, M.E., MacLeod, A.M., Snyder, A.Z., Powers, W.J., Gusnard, D.A., Shulman, G.L., 2001. A default mode of brain function. Proc. Natl. Acad. Sci. 98, 676.
Rostrup, E., Law, I., Blinkenberg, M., Larsson, H.B., Born, A.P., Holm, S., Paulson, O.B., 2000. Regional differences in the CBF and BOLD responses to hypercapnia: a combined PET and fMRI study. NeuroImage 11, 87–97.
Saad, Z.S., Ropella, K.M., Cox, R.W., DeYoe, E.A., 2001. Analysis and use of FMRI response delays. Hum. Brain Mapp. 13, 74–93.
Seeley, W.W., Menon, V., Schatzberg, A.F., Keller, J., Glover, G.H., Kenna, H., Reiss, A.L., Greicius, M.D., 2007. Dissociable intrinsic connectivity networks for salience processing and executive control. J. Neurosci. 27, 2349–2356.
Seifritz, E., Esposito, F., Hennel, F., Mustovic, H., Neuhoff, J.G., Bilecen, D., Tedeschi, G., Scheffler, K., Di Salle, F., 2002. Spatiotemporal pattern of neural processing in the human auditory cortex. Science 297, 1706–1708.
Shannon, B.J., Buckner, R.L., 2004. Functional-anatomic correlates of memory retrieval that suggest nontraditional processing roles for multiple distinct regions within posterior parietal cortex. J. Neurosci. 24, 10084–10092.
Smith, S.M., Miller, K.L., Moeller, S., Xu, J., Auerbach, E.J., Woolrich, M.W., Beckmann, C.F., Jenkinson, M., Andersson, J., Glasser, M.F., Van Essen, D.C., Feinberg, D.A., Yacoub, E.S., Ugurbil, K., 2012. Temporally-independent functional modes of spontaneous brain activity. Proc. Natl. Acad. Sci. U. S. A. (online early).
Sridharan, D., Levitin, D.J., Menon, V., 2008. A critical role for the right fronto-insular cortex in switching between central-executive and default-mode networks. Proc. Natl. Acad. Sci. U. S. A. 105, 12569–12574.
Teipel, S.J., Bokde, A.L., Meindl, T., Amaro, E.J., Soldner, J., Reiser, M.F., Herpertz, S.C., Moller, H.J., Hampel, H., 2010. White matter microstructure underlying default mode network connectivity in the human brain. NeuroImage 49, 2021–2032.
Uddin, L.Q., Kelly, A.M., Biswal, B.B., Xavier Castellanos, F., Milham, M.P., 2009. Functional connectivity of default mode network components: correlation, anticorrelation, and causality. Hum. Brain Mapp. 30, 625–637.
van den Heuvel, M., Mandl, R., Luigjes, J., Hulshoff Pol, H., 2008. Microstructural organization of the cingulum tract and the level of default mode functional connectivity. J. Neurosci. 28, 10844–10851.
Weiskopf, N., Veit, R., Erb, M., Mathiak, K., Grodd, W., Goebel, R., Birbaumer, N., 2003. Physiological self-regulation of regional brain activity using real-time functional magnetic resonance imaging (fMRI): methodology and exemplary data. NeuroImage 19, 577–586.
Weissman, D.H., Roberts, K.C., Visscher, K.M., Woldorff, M.G., 2006. The neural bases of momentary lapses in attention. Nat. Neurosci. 9, 971–978.